Journal of the Serbian Chemical Society
JSCS-info@shd.org.rs • www.shd.org.rs/JSCS
J. Serb. Chem. Soc. 81 (10) 1199–1213 (2016)
JSCS–4919
UDC 504.4.054+546.19:541.183+546.722–31'44:676:66.017
Original scientific paper

Efficient pollutants removal by amino-modified nanocellulose impregnated with iron oxide

KHALED A. TALEB[1], JELENA D. RUSMIROVIĆ[2], MILICA P. RANČIĆ[3#], JASMINA B. NIKOLIĆ[1#]*, SAŠA Ž. DRMANIĆ[1#], ZLATE S. VELIČKOVIĆ[4] and ALEKSANDAR D. MARINKOVIĆ[1#]

[1]*Department of Organic Chemistry, Faculty of Technology and Metallurgy, University of Belgrade, Karnegijeva 4, 11120 Belgrade, Serbia,* [2]*Innovation center, Faculty of Technology and Metallurgy, Karnegijeva 4, 11120 Belgrade, Serbia,* [3]*Faculty of Forestry, University of Belgrade, Kneza Višeslava 1, 11030 Belgrade, Serbia and* [4]*Military Academy, University of Defence, 33 General Pavle Jurišić-Šturm Street, Belgrade, Serbia*

(Received 29 May, revised 14 June, accepted 15 June 2016)

Abstract: A novel adsorbent, NC-PEG, obtained by modification of nanocellulose (NC) with PEG-6-arm amino polyethylene glycol (PEG-NH_2) *via* maleic anhydride (MA) linker, was used for removal of Cd^{2+} and Ni^{2+} from water. A subsequent precipitation of iron oxide (FO) from goethite on NC-PEG was employed to produce NC-PEG/FO adsorbent which was used for As(V) and As(III) removal. In a batch test, the influence of pH, contact time, initial ion concentration and temperature on the adsorption efficiency were studied. The maximum adsorption capacities found for Cd^{2+} and Ni^{2+}, obtained by the use of Langmuir model, were 37.9 and 32.4 mg g^{-1} at 25 °C, respectively. Also, high As(V) and As(III) removal capacities of 26.0 and 23.6 mg g^{-1} were obtained. The thermodynamic parameters indicated endothermic, feasible and spontaneous nature of the adsorption process. The kinetic study, *i.e.*, fitting by Weber–Morris model predicted that intra-particle diffusion was the rate-controlling step. The ability for multi-cycle reusability of both NC-PEG and NC-PEG/FO, represents a positive indicator when considering their possible applications.

Keywords: arsenic; adsorption; hydrous iron oxide; nanocellulose.

INTRODUCTION

Arsenic is a common element, natural component of the earth's crust, generally found in trace quantities in rocks, soil, water and air. However, human

* Corresponding author. E-mail: jasmina@tmf.bg.ac.rs
# Serbian Chemical Society member.
doi: 10.2298/JSC160529063T

activities such as agricultural and industrial processes, the use of arsenic herbicides, crop desiccants, and pesticides, petroleum refining and combustion of fossil fuels also contribute to the growing arsenic contamination of the ground and surface water. Since arsenic is classified as a Class A human carcinogen,[1,2] the United State Environmental Protection Agency and the World Health Organization decreased the maximum contaminant level (MCL) of arsenic from 50 to 10 μg dm^{-3}.[3] The growing concern about the environmental contamination has initiated an extensive research and development of safe technologies for effective arsenic removal.

The adsorption is considered as a simple, efficient, highly effective and environmentally friendly method for removal of heavy metals from aqueous solutions.[4–7] The adsorption process represents an accumulation of gas or liquid solute on the surface of the adsorbent and formation of a molecular or atomic film on the adsorbate. The preferred adsorbents should be thermostable, highly porous, amorphous solids consisting of microcrystallites with good balance between micro- and macropores.[5,8] Recently, different natural macromolecules such as cellulose,[9,10] chitosan, starch, and alginate were applied for adsorbing heavy metal ions from wastewater.[5]

As one of the most abundant biopolymers in nature, which is environmentally friendly, biocompatible and renewable material, the cellulose has a huge potential for production of various functional, sustainable and biodegradable materials.[11] The increasing interest in nanomaterials of a plant origin and their unique properties led to extensive research of nanocellulose materials. The nanocellulose combines important cellulose properties such as hydrophilicity, wide chemical-modification capacity, and the ability to form versatile semicrystalline fiber morphologies with the specific features of the nanoscale materials caused by their large surface area.[12] Since the native cellulose consists of crystalline and amorphous regions, when cellulosic fibers were subjected to intensive acid treatment, the amorphous parts break up and cellulose nanocrystals (NCs) can be extracted.[13] The presence of numerous hydroxyl groups on the NC surface make this biopolymer suitable for chemical modification and introduction of various specific groups such as amino and carboxyl groups. Therefore, the functional nanosized cellulose represents a high adsorption capacity material suitable for removal of heavy metal ions from aqueous solution.[14–16]

The goal of this study was focused on the design of effective, reusable modified nanocellulose based adsorbents: nanocellulose (NC) modified by PEG-6--arm amino polyethylene glycol, PEG-NH_2 (NC-PEG), and NC-PEG subsequently modified by precipitation iron oxide (FO) from goethite (NC-PEG/FO), applicable for removal of heavy metals. In order to produce a NC-PEG adsorbent, the modification of the NC surface with maleic acid anhydride (MA), in the first step, was followed by a reaction with PEG-NH_2 in order to introduce amino

terminal PEG branched organic structure. In this way an efficient adsorbent, NC--PEG, for Cd^{2+} and Ni^{2+} removal was obtained. The precipitation from goethite form FO on NC-PEG, which is performed according to an optimized procedure, produced NC-PEG/FO adsorbent applicable for As(V) and As(III) removal. The specific objectives of the presented work were to study the performance of both adsorbents in terms of: 1) textural and morphological properties; 2) adsorption efficiency; 3) capacity, and 4) kinetics/diffusional processes.

EXPERIMENTAL

Materials

Full description of the used materials is given in the Supplementary material to this paper.

Adsorbents preparation

The experimental methodology applied for nanocellulose (NC) isolation,[17] subsequent modification with maleic anhydride (MA)[18] to produce NC-MA, and NC-MA modification with PEG-6-arm amino polyethylene glycol (PEG-NH_2) to prepare NC-PEG adsorbent is given in the Supplementary material to this paper.

Precipitation of iron oxide (FO) on NC-PEG

NC-PEG (10 g) was sonicated in DI water (30 cm^3) with simultaneous introduction of N_2 for 30 min. The reaction was conducted continuously, under magnetic stirring and inert atmosphere, by drop-wise addition of 83 cm^3 $FeSO_4 \cdot 7H_2O$ solution with concentration of 0.05, 0.1, 0.15, 0.2, 0.25, 0.3 and 0.35 mol dm^{-3}, respectively, from dropping funnel for 15 min. The ferri/ferro oxidation was performed by changing the nitrogen with air introduction, and neutralizing the reaction mixture by addition of 75 cm^3 sodium bicarbonate with different concentration: 0.1, 0.2, 0.3, 0.4 and 0.5 mol dm^{-3} for 30 min, which caused the precipitation of iron oxide into goethite form.[19] The reaction was conducted for 48 h until the green-blue color of the solution changed to ocher shade. The obtained product was filtered, washed with DI water, and freeze-drying was conducted by cooling and keeping the freshly obtained material at –30 °C for 24 h, followed by freeze-drying at –50 °C and pressure of 0.05 mbar for 24 h, and final treatment of the material at –70 °C and 0.01 mbar for 1 h. The procedure for the precipitation of FO was repeated in an analogous manner, and the obtained adsorbent was named NC-PEG/FO.

Optimization of the adsorbent preparation

The optimization of the adsorbent synthesis was performed by using response surface methodology (RSM)[20,21] and was based on three-level-two-factor central rotatable composite design (blocked single factor: temperature).[22,23]

The details related to the optimization, description of adsorption and kinetic experiments in a batch system and adsorption data modeling and statistical analysis are given in the Supplementary material.

RESULTS AND DISCUSSION

The XRD analysis

The crystal structure of goethite was determined by using XRD technique. Increase in the crystallinity after modification of NC with maleic acid anhydride

(Fig. S-2 of the Supplementary material to this paper) was shown in a recent publication.[18] Both NC and NC-MA diffractograms displayed well-defined doublet peaks for the (200) plane of cellulose with the first peak at 2θ 20° and the second at 2θ 22° which indicated the existence of cellulose I and cellulose II allomorphs. The signal at 2θ 35°, having higher intensity in the diffractogram of the NC-MA sample, corresponded to (004) atomic plane of cellulose I.

The XRD pattern of NC-PEG/FO is shown in Fig. 1. The analysis showed characteristic peaks corresponding to amorphous goethite observed at 2θ value of 21.2, 33.2, 36.6 and 53.2° (ICDD PDF2 No. 81-0464). The XRD patterns showed large scattering due to the small crystallite size and amorphous properties of the precipitated goethite.

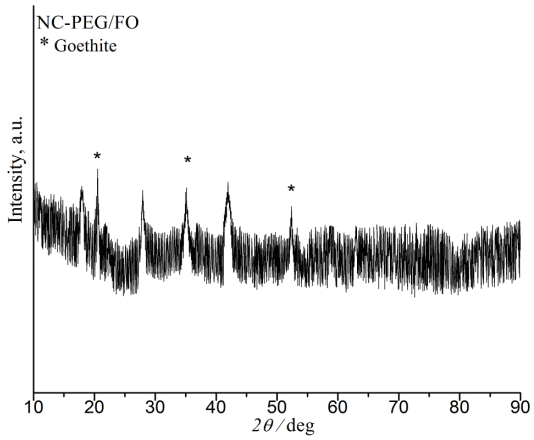

Fig. 1. XRD pattern of NC-PEG/FO.

Textural properties and pH_{PZC} of the synthesized adsorbents

A multi-step adsorbent synthesis was performed in order to produce adsorbent material with an appropriate geometry, morphology and porosity. The determined values of the textural properties and point of zero charge values (pH_{PZC}) are summarized in Table I.

TABLE I. Textural properties and pH_{PZC} of the studied adsorbents

Adsorbent	Specific surface area $m^2 g^{-1}$	Pore volume $cm^3 g^{-1}$	Pore diameter nm	pH_{PZC} [a]	pH_{PZC} [b]
NC-PEG	38.7	0.72	17.4	6.9	6.4
NC-PEG/FO	62.1	0.80	26.4	8.5	7.6

[a]Before and [b]after adsorption; pH_{PZC} of NC < 1, and pH_{PZC} of NC-MA < 3

It was found that the cations were strongly bonded to amino groups, by complexation/chelation interactions, and the higher nucleophilicity of the amino groups, at pH higher than pH_{PZC}, led to stronger interaction with cadmium and nickel cations.[24,25]

Due to different properties of NC (32.4 m^2 g^{-1}) and the synthesized materials, higher values for the specific surface area were obtained for both NC-PEG and NC-PEG/FO. Additionally, the shift of the pH_{PZC} value indicated specific arsenate adsorption rather than electrostatic interaction,[25–27] as well as formation of complexed/precipitated arsenic species at the surface of the goethite based adsorbent. The determination of the iron content in an acidic extract, obtained by using 10 % nitric acid and microwave digestion, showed that 11.7 % of the iron was precipitated in goethite form at the NC-PEG surface.

Morphological characterization

The morphology of both materials indicated surface coverage by organic material. The chemical treatment followed by FO deposition affected the morphological structure of the surface of NC-PEG/FO (Fig. 2). The evolution of the NC-PEG/FO morphology could be explained by the heterogeneous reaction between FO and the terminal amino-branched structures at the NC-PEG grains.

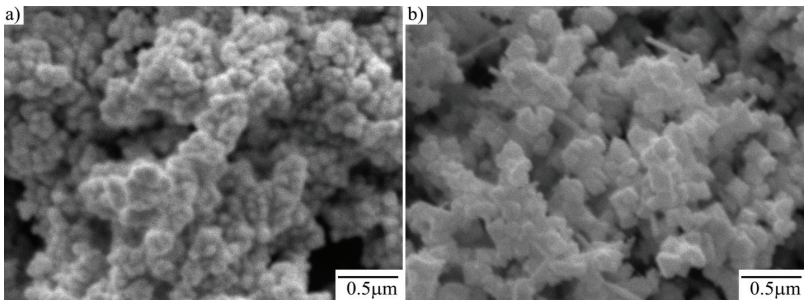

Fig. 2. SEM images of NC-PEG (a) and NC-PEG/FO (b).

FTIR analysis

The analysis of FTIR spectra provided information about the bonding interactions between the adsorbate and the adsorbent's functional groups. The change in the vibration frequency, caused by adsorbate/adsorbent group interactions was a result of the bond strength change. The band shift to lower or higher frequencies indicated bond weakening or strengthening, respectively. The FTIR spectra of both adsorbents recorded before and after arsenate adsorption at 3 mg dm^{-3} concentration of Cd^{2+} and As(V) are shown in Fig. 3. The lower concentration did not lead to significant change in the absorption frequencies of the bands of interest. An analysis of the FTIR spectra of NC-PEG showed presence of a weak band at ≈1640 cm^{-1} which could be assigned to stretching of the amide carbonyl (C=O) overlapping with OH bending vibration. In addition, the bands at ≈1430 and 1150 cm^{-1}, correspond to N–H in-plane and C–N bond stretching vibration, respectively. The broad peaks at 3300–3600 cm^{-1} were due to the NH_2 stretch of the amine group overlapped with OH vibration.

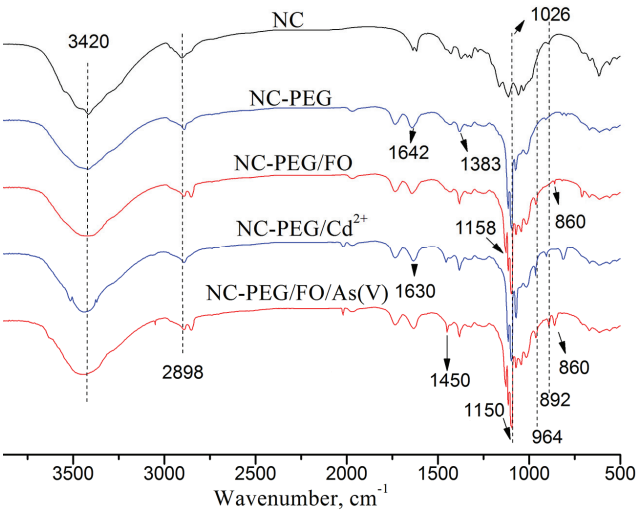

Fig. 3. FTIR spectra of NC, NC-PEG, NC-PEG/FO, NC-PEG/Cd^{2+} and NC-PEG/FO/As(V).

Also, the broad bands at ≈1680 and ≈1630 cm^{-1}, assigned to a carbonyl amide stretching vibration (amide I) and N–H in-plane vibration, respectively, was not significantly affected by the interaction with the increased cation concentration (Fig. 3). In addition, the bands at ≈1158 and ≈860 cm^{-1}, corresponding to C–N stretching and out-of-plane NH_2 bending mode (twisting), respectively, almost completely disappeared. The role of the primary amino group to bonding of Cd^{2+} was observed in a significantly higher adsorption capacities.[24] This indicated that the positively charged cation had a pronounced influence on the electronic density at the amino group, and this interaction of Cd^{2+} with the amino lone pair restricted the N–H out-of plane movement with appropriate restriction of the N–H in-plane vibrations. Analogous and similar analysis stands for the FTIR spectra of NC-PEG/Ni^{2+} (not shown) at different nickel cation loading.

The adsorption properties of the FO in the NC-PEG/FO adsorbent are mainly due to the existence of OH_2^+, OH and O^- functional groups at the adsorbent surface. The iron oxide surface, exposed to water at different pH, developed surface charges and by adsorbing metal ions completed the coordination shells with OH groups, which either bound to or released H^+. At neutral and acidic pH (less than 8), the OH_2^+ and OH groups on the goethite surface were dominant and responsible for the selective binding of molecular and ionic forms of arsenic species.[24,27] Differences in the spectra before and after As(V) adsorption could be noticed. The broad band at ≈3420 cm^{-1}, ascribed to OH and NH_2 stretching vibrations, asymmetric and symmetric, was not significantly affected by the adsorbed pollutant. According to the FTIR spectra of NC-PEG/FO and NC-PEG/FO/ /As(V), it can be observed a low weakening of the Fe–OH bands (peaks at 1126,

1043 and 964 cm^{-1}) as well as appearence of new peaks at 892 and 860 cm^{-1} in the NC-PEG/FO/As(V) spectrum originated from As–O stretching vibration of coordinated arsenic species (using As(V) concentration > 2 ppm).[24,27] This could be explained with the fact that the As–O–Fe bond strength increased with increasing of the coordination number. Consequently, the wavelength of the stretching vibration of the uncomplexed/unprotonated As–O–Fe was located at a higher value (892 cm^{-1}), while the one of the complexed As–O–Fe band was located at a lower frequency (860 cm^{-1}).

Effect of pH on the adsorption efficiency

The pH influences the equilibrium of ionic species and protonation/deprotonation of the sorbent functional groups. It is known that the presence of hydrogen/hydroxide ions could modify the redox potential of both sorbate and sorbent, and provoke dissolution of the sorbent. The degree of As(V), As(III), Cd^{2+} and Ni^{2+} removal *vs.* initial pH (pH_i), in presence of the studied adsorbents, are presented in Fig. 4.

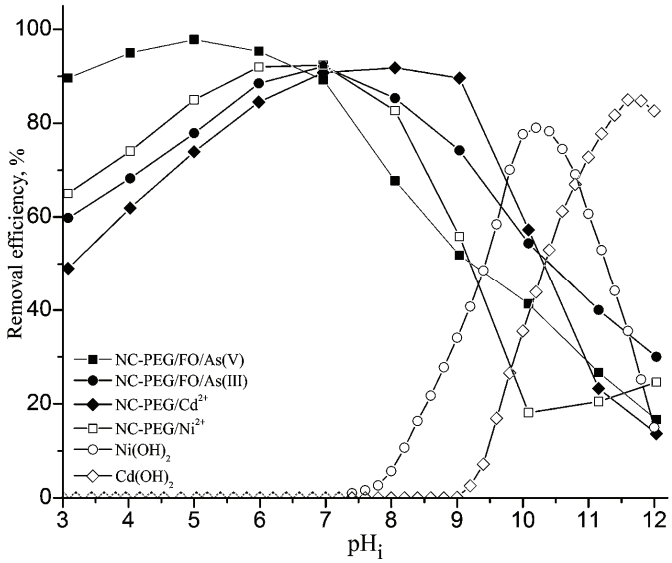

Fig. 4. Influence of pH on As(V) and As(III) removal by NC-PEG/FO, and Cd^{2+} and Ni^{2+} removal by NC-PEG (c_i = 100 μg dm^{-3}, m/V = 100 mg dm^{-3}, t = 25 °C).

It could be noted from Fig. 4 that the percentage of As(V) and As(III) adsorption on NC-PEG/FO at pH 7 was >90 %, and subsequently, a gradual decrease started at pH > 7. According to pH-dependent ionization of triprotic arsenic and arsenous acid, the highest adsorption capacity showed the most effective removal at pH in vicinity of pK_a.[28,29] The charged As species participated in different electrostatic interactions (attraction/repulsion) with surface/ions charges

thus influencing the intensity of the As flux toward the specific adsorption sites. The positively charged surface of NC-PEG/FO adsorbent at pH < pH_{PZC}, attracted the negatively charged arsenate causing higher intensity of the As flux toward the adsorbent surface. The opposite was valid at higher pH. The selection of optimal pH 6 was dictated by three factors: adsorption capacity, adsorbent deposit stability (dissolution) and consideration of the techno-economic indicator.

In order to eliminate the possible effect of the precipitation of $Cd(OH)_2$ and $Ni(OH)_2$, quantitative determinations of the precipitate were performed without addition of NC-PEG.[24,28] The results indicated significant precipitation of $Cd(OH)_2$ at pH > 9 and of $Ni(OH)_2$ at pH > 7.5 (Fig. 4).

According to the data at pH < 8, it is clear that the Cd^{2+} and Ni^{2+} removal was not affected by the salt precipitation. Thus, the pH-dependent adsorption profiles (Fig. 4) for NC-PEG/Cd^{2+} and NC-PEG/Ni^{2+} presented differences between the overall pollutant removal and precipitated salt. In that sense, the optimal pH for all pollutant removal was chosen to be pH 6. A lower pH could have detrimental effect on the organic functionalities or could cause increase in the solubility of FO nanoscale deposit in the NC-PEG/FO adsorbent. Moreover, the pH of 5–6.5 is usually found in most natural waters, which means that the implementation of such technology could have positive techno-economic indicators.

Adsorption study: pollutants removal by NC-PEG and NC-PEG/FO

Considering the significant influence of pH on the pollutant speciation and ionization state of adsorbent surface, it was important to study the influence of pH, in the range 3–10, on the effectiveness of the pollutant removal. The amino groups contributed to an increase in the surface basic properties and, thus, according to the pH_{PZC} value of NC-PEG (6.9), preferable electrostatic interactions favored the adsorption of cations at pH > pH_{PZC}. Due to the need of pH adjustment in order to reach pH > pH_{PZC} and to change significantly the ionic strength of the solution, the optimal pH 6 was selected and applied during cations removal. It was shown in a previous work that the optimal pH for As(V) removal in a presence of goethite modified macroporous resin was 6–6.5, and this value was used in the present work.[26,27]

The adsorption capacity was evaluated by using a non-linear regression method with commonly used isotherm models: Langmuir, Freundlich, Redlich–Peterson and Dubinin–Radushkevich (D–R). The highest correlation coefficients were obtained by using the D–R equation for NC-PEG and Freundlich model for NC-PEG/FO (the data are given in Fig. S-3 and Table S-II of the Supplementary material). According to the Freundlich isotherm, the mechanism of cations adsorption onto NC-PEG could be described by heterogenous adsorption, where the adsorbed ions/molecules had different enthalpies and adsorption activation energies. The *n* value from the Freundlich isotherm is a measure of the

adsorption intensity or surface heterogeneity. Values of n close to zero indicate a highly heterogeneous surface. Whereas a value of $n < 1$ implies chemisorption process, the higher value is an indication of cooperative adsorption, *i.e.*, physisorption and chemisorption, with different contribution at different steps of the equilibration of the system. Values of $n > 1$ indicate slight decrease in the intensity of the adsorption processes at lower sorbate concentration, and also indicate the presence of different active centers where the centers with the highest energy have a higher activity, *e.g.*, participate in the initial adsorption step.

The D–R isotherm model is mainly valid at low pollutant concentration, and is usually used for description of adsorption on both homogeneous and heterogeneous surfaces.[25]

The maximum adsorption capacities for As(V) and As(III) using NC-PEG/ /FO as well as for Cd^{2+} and Ni^{2+} removal by NC-PEG, as obtained by Langmuir model, are given in Table II.

TABLE II. Maximum adsorption capacities (q_e / mg g^{-1}) for As(V), As(III), Cd^{2+} and Ni^{2+} obtained by Langmuir model

Adsorbent	Ion	t / °C		
		25	35	45
NC-PEG/FO	As(V)	26.0	27.4	28.6
	As(III)	23.6	24.3	25.5
NC-PEG	Cd^{2+}	37.9	40.9	43.9
	Ni^{2+}	32.4	33.7	35.0

The results of fitting the experimental data by Langmuir isotherm showed a high predicted adsorption capacity for As(V), and an increase in the adsorption capacity with increase of the temperature: from 26.0 mg g^{-1} at 25 °C and 27.4 mg g^{-1} at 35 °C to 28.60 mg g^{-1} at 45 °C. The maximum adsorption capacities of As(III), Cd^{2+} and Ni^{2+}, obtained by using the Langmuir model, showed similar trend of increase (Table II).

The separation factor (K_R) describes whether or not a sorption system is favorable and can be expressed by Eq. (1):

$$K_R = \frac{1}{1 + bc_0} \quad (1)$$

where c_0 is the initial concentration (mg L^{-1}) and b is the Langmuir constant (L mg^{-1}). According to the value of K_R, the adsorption can be described as unfavorable ($K_R > 1$), linear ($K_R = 1$), favorable ($0 < K_R < 1$) or irreversible ($K_R = 0$).[29] The obtained values of K_R are in the range from 0.0095 to 0,865 and indicated favorable adsorption of the investigated adsorbate on both NC-PEG and NC--PEG/FO adsorbents.

Adsorption kinetics

The determination of the adsorption rate by which the system attains equilibrium could help for a better understanding of the pollutant adsorption mechanism, *i.e.*, probable reaction pathways. Due to the complexity of the adsorption process, *e.g.*, complex adsorption steps with contribution of mass transfer and chemical reaction processes, different kinetic models were used to fit the experimental data. The kinetic data were analyzed by non-linear least-squares method in the form of pseudo-first, pseudo-second-order (PSO) rate equations and intra-particle diffusion model (Weber–Morris model, W–M). Judging from the regression coefficients, the kinetic data were satisfactorily fitted by using pseudo-second-order (PSO) equation.[24,25] The kinetic parameters obtained from the PSO equation for Cd^{2+}, Ni^{2+} and arsenic removal at 25 °C are given in Table III.

TABLE III. Kinetic parameters for the investigated adsorbate removal at 25 °C obtained by the use of PSO equation c_i = 1 mg dm^{-3} for As(V) and As(III), and 0.5 mg dm^{-3} for Cd^{2+} and Ni^{2+}

Parameter	NC-PEG/FO		NC-PEG	
	As(V)	As(III)	Cd^{2+}	Ni^{2+}
k_2 / g mg^{-1} min^{-1}*	0.054	0.063	0.037	0.050
q_e / mg g^{-1}	4.419	4.384	8.488	4.391
R^2	0.998	0.997	0.999	0.998

The activation energy for pollutants removal was calculated using Arrhenius Equation. The calculated activation energies for As(V) and As(III) adsorption on NC-PEG/FO were found to be 9.58 and 15.46 kJ mol^{-1}, respectively. The obtained activation energies for Cd^{2+} and Ni^{2+} adsorption on NC-PEG were 2.67 and 6.94 kJ mol^{-1}, respectively. These results are in agreement with a study of As(V) adsorption on synthetic goethite presented in the work of Lakshmipathiraj *et al.*[30] The authors in previous reseach stated that intra-particle diffusion was the rate-controlling step in the case of activation energy lower and within the range of 8–22 kJ mol^{-1}, which is characteristic for diffusion-controlled processes such as ion-exchange/complexation.[31]

The results from the use of PSO equation provided fitting of the kinetic parameters related to the overall adsorption rate, and could not help in assessing the rate-limiting step. Therefore, the intra-particle diffusion model,[24] *i.e.*, the Weber–Morris (W–M) model, was applied to analyze the mass transfer phenomena of the overall process, and the results are given in Table IV. The adsorption is usually accomplished through a series of distinct consecutive steps: external mass transfer (diffusion through the bulk liquid), diffusion across boundary layer surrounding the particle (film diffusion), diffusional transport within the internal structure of the adsorbent (intra-particle diffusion) and adsorption on the solid surface. Regardless of the simplicity of the W–M model, it suffers from uncert-

ainties caused by the multi-linear nature, *i.e.*, the overall mass transport could be controlled by more than one step at different stages of the adsorption process.

TABLE IV. Kinetic parameters of the W–M model for arsenate adsorption

Step	Parameter	NC-PEG/FO		NC-PEG	
		As(V)	As(III)	Cd^{2+}	Ni^{2+}
1	k_{p1} / mg g^{-1} $min^{-0.5}$	0.262	0.130	0.281	0.159
	c_1 / mg g^{-1}	2.467	3.099	4.891	2.387
	R^2	0.999	0.997	0.998	0.997
2	k_{p2} / mg g^{-1} $min^{-0.5}$	0.118	0.078	0.0892	0.142
	c_2 / mg g^{-1}	3.099	3.340	7.317	2.891
	R^2	0.997	0.999	0.979	0.999
3	k_{p3} / mg g^{-1} $min^{-0.5}$	0.033	0.0033	0.0577	0.020
	c_3 / mg g^{-1}	3.930	3.931	7.651	4.025
	R^2	0.969	0.971	0.985	0.997

The results obtained by using the Weber–Morris model showed three successive linear steps: fast kinetic in the first step followed by medium to low adsorption rate in the second and third steps. The intercept c_1 found for the first step indicated a higher resistance, *i.e.*, slower ionic transport, due to the intra-particle diffusion, whereas the k_{p1} value demonstrated external mass transfer from the bulk solution to the most available outer adsorbent surface adsorptive sites. The second part of the W–M fit represented processes which highly depended on the adsorbent porosity, *i.e.*, pore geometry and network density. Due to the concentration gradient the ions diffuse through the bulk solution and tree-like system of macro-, meso- and micropores extending into the adsorbent interior to reach all available surface active sites.[24] The intra-particle and film diffusion resistance slowed down the adsorbate transport, *i.e.*, net transport in a direction of variable time-dependent concentration gradient. At the final stage of the process, the adsorption took place at low rate until saturation of all available surface sites was achieved. Additional analysis on the contribution of external mass transfer and diffusion inside the pores to overall diffusional adsorbate transport was also performed.

Thermodynamic study

The temperature effect on the pollutants adsorption onto NC-PEG and NC--PEG/FO, respectively, was deduced from the results of the adsorption experiments performed at 25, 35 and 45 °C. The temperature dependence of arsenic adsorption was associated with changes in the thermodynamic parameters such as adsorption equilibrium constant, K_L, $\Delta G^{\ominus}$ (the standard Gibb's free energy change), $\Delta H^{\ominus}$ (the standard enthalpy change), and $\Delta S^{\ominus}$ (the standard entropy change).[24,25] The obtained results are given in Table V.

The negative values of $\Delta G^{\ominus}$ indicated a spontaneous process and more beneficial adsorption at higher temperature, while the positive $\Delta H^{\ominus}$ additionally con-

firmed the conclusion about more effective adsorption at higher temperature (Table VI). Somewhat higher enthalpy was obtained for Cd^{2+} and Ni^{2+} adsorption, which means more preferable adsorption for both adsorbates at higher temperature. Lower values, 5.17 and 5.25 kJ mol^{-1}, were obtained for As(V) and As(III) removal with NC-PEG/FO, respectively. The breakage of water hydration shells by the pollutant species and their transport through the bulk solution, within the pores and through the surface boundary layer was more intensive process at a higher temperature. The transport of exchangeable pollutant ions to the adsorption sites and the release of a number of water (exchangeable) molecules into the bulk solution contributed to the increase in the entropy change.[24,25] At steady-state conditions, the randomness at the adsorbent/solution interface was increased due to different intermolecular interactions which contributed to positive entropy change, *i.e.*, the adsorption is an entropy-driven process. All of these elementary processes, which took place in the course of equilibrium attainment, contributed to the positive enthalpy change.

TABLE V. Thermodynamic parameters of adsorption processes of As(V), As(III), Cd^{2+} and Ni^{2+}

Adsorbent	Ion	t °C	$\Delta G^{\ominus}$ kJ mol^{-1}	$\Delta H^{\ominus}$ kJ mol^{-1}	$\Delta S^{\ominus}$ J mol^{-1} K^{-1}	K_L L mol^{-1}	R^2
NC-PEG/FO	As(V)	25	–39.2	5.17	114.19	132668	0.938
		35	–40.41			127823	
		45	–41.48			116277	
	As(III)	25	–39.58	5.25	115.13	154724	0.999
		35	–40.72			144217	
		45	–41.88			135449	
NC-PEG	Cd^{2+}	25	–43.16	8.30	117.92	657828	0.994
		35	–44.30			581930	
		45	–45.50			533167	
	Ni^{2+}	25	–44.21	9.39	116.77	55678545	0.998
		35	–45.36			48895732	
		45	–46.54			43785090	

Regeneration and reusability

The design of an environmentally friendly and economically acceptable technology for pollutant removal necessarily demands the development of long-term adsorbent applications. The number of the re-use cycles of the adsorbent contributes to the effectiveness of overall technology. The selection of an efficient reagent for the regeneration depended on the cations and arsenic bonding type, nature of sorbent, amino groups at the surface of NC-PEG and hydroxyl groups at the surface of NC-PEG/FO. The formation of surface complexes, monodentate, bidentate-mononuclear and bidentate-binuclear through As–O–Fe bond, indicated the necessity of application of strong competitive anion capable

to break the As–O–Fe bond, *i.e.*, to displace the As(V) anion.[27] On the other hand, the Lewis acid complexes, Cd^{2+} and Ni^{2+}, and terminal amino groups present on the NC-PEG surface could be easily desorbed by using a stronger inorganic base.[24] Therefore, the objective of the competitive cation and anion exchange from the adsorbent surface was their release into the solution leaving the concentration of the active surface sites at the level, as close as possible, to the one before the adsorption cycle. A subsequent rinsing of the NC-PEG/FO adsorbent with dilute 2 % sulfuric acid, caused protonation of the negatively charged surface functional groups, thus providing their sorption potential. Many systems for regeneration were used, and it was found that the most efficient one was NaOH/NaCl. The results from the desorption study are presented in Table VI.

TABLE VI. Results of arsenate desorption from NC-PEG and NC-PEG/FO in first cycle by NaOH/NaCl

c / mol dm^{-3}	NC-PEG/FO		NC-PEG	
	As(V)	As(III)	Cd^{2+}	Ni^{2+}
0.2/0.2	79	80	78	79
0.5/0.2	87	88	83	85
0.5/0.5	92	94	88	91

Small decrease in the adsorption capacity was observed over five adsorption/regeneration cycles (in the range of 10–25 %). The most efficient desorption system was found to be the NaOH/NaCl (0.5/0.5) system. In the first cycle 92 % of the As(V) were desorbed, and throughout five consecutive cycles, the desorption efficiency decreased to 80 % in the fifth desorption cycle for the NC-PEG/FO adsorbent. Similarly the results for As(III) showed 94 % desorption efficiency in the first and 82 % in fifth desorption cycle. The desorption efficiency for Cd^{2+} and Ni^{2+} from the NC-PEG adsorbent were: 88 and 91 % in first and 79 and 77 % in fifth desorption cycle, respectively. In summary, the NC-PEG and NC-PEG/FO are reusable in a multi-step processes and efficient adsorbents for Cd^{2+} and Ni^{2+}, as well as for As(V) and As(III) oxyanions removal for over five adsorption/desorption cycles.

CONCLUSIONS

In the present work, the highly efficient adsorbents for As(V), As(III), Cd^{2+} and Ni^{2+} removal were obtained by the impregnation of goethite on amino modified NC. The best adsorption performance of NC-PEG and NC-PEG/FO was discussed as a consequence of the adsorbent specific surface area, mesopore volume and diameter, as well as of their hybrid nature. The use of adequate statistical analysis and proper selection of the isotherm model, *i.e.*, Freundlich and Dubinin–Radushkevich models, led to the best correlation of the adsorption data. The best fitting of the kinetic data was obtained by the use of pseudo-sec-

ond-order and Weber–Morris kinetic models, which showed that the intra-particle diffusional transport is a limiting step. The thermodynamic parameters revealed that the adsorption processes were favorable and more spontaneous at a higher temperature. The experimental results showed that the used adsorbents were efficient and reusable for cations and As(V) removal from natural water in the batch mode. In summary, this paper described the role of a multistep adsorbent synthesis in order to obtain the novel environmentally friendly adsorbent material NC-PEG as high performance adsorbent for Cd^{2+} and Ni^{2+} removal. Also, an additional modification of the NC-PEG adsorbent by goethite precipitation produced NC-PEG/FO adsorbent applicable for As(V) and As(III) removal.

SUPPLEMENTARY MATERIAL

Experimental details, additional characterization data, optimization procedure, some XRD data and adsorption isotherms are available electronically at the pages of journal website: http://www.shd.org.rs/JSCS/, or from the corresponding author on request.

Acknowledgements. The authors acknowledge financial support from Ministry of Education, Science and Technological development of the Republic of Serbia, Project No. 172013, and University of Defence, Republic of Serbia, project VA-TT/4/16-18.

ИЗВОД

ЕФИКАСНО УКЛАЊАЊЕ ПОЛУТАНАТА ПОМОЋУ АМИНО-МОДИФИКОВАНЕ НАНОЦЕЛУЛОЗЕ ИМПРЕГНИСАНЕ ГВОЖЂЕ-ОКСИДОМ

KHALED A. TALEB[1], ЈЕЛЕНА Д. РУСМИРОВИЋ[2], МИЛИЦА П. РАНЧИЋ[3], ЈАСМИНА Б. НИКОЛИЋ[1], САША Ж. ДРМАНИЋ[1], ЗЛАТЕ С. ВЕЛИЧКОВИЋ[4] и АЛЕКСАНДАР Д. МАРИНКОВИЋ[1]

[1]Катедра за органску хемију, Технолошко–металуршки факултет, Универзитет у Београду, Карнегијева 4, п.пр. 3503, 11120 Београд, [2]Иновациони центар, Технолошко–металуршки факултет, Карнегијева 4, п.пр. 3503, 11120 Београд, [3]Шумарски факултет, Универзитет у Београду, Кнеза Вишеслава 1, 11030, Београд и [4]Војна Академија, Универзитет одбране, Генерала Павла Јуришића-Штурма 33, Београд

Нови адсорбент, NC-PEG, добијен модификацијом наноцелулозе (NC) са PEG-6-arm амино-полиетилен-гликолом (PEG-NH_2) преко малеин-анхидридног остатка (MA), је коришћен за уклањање Cd^{2+} и Ni^{2+} из воде. Таложење гвожђе оксида (FO) на NC-PEG у наредном кораку даје NC-PEG/FO адсорбент који је коришћен за уклањање As(V) и As(III) јона. Утицај pH, времена контакта, почетне концентрације јона, на ефикасност адсорпције је испитивана у шаржном систему. Максимални адсорпциони капацитет за Cd^{2+} и Ni^{2+}, добијен применом Langmuir модела, је 37,9 и 32,4 mg g^{-1}, редом, на 25 °C. Такође, висок степен уклањања As(V) и As(III) јона је констатован на основу максималног адсорпционог капацитета који је износио 26,0 и 23,6 mg g^{-1}, редом. Термодинамички параметри процеса адсорпције указују на ендотерман, изводљив и спонтан процес адсорпције. Кинетичка испитивања, тј. моделовање адсопционог процеса применом Weber–Morris модела предвиђа унутарчестичну дифузију као корак који одређује укупну брзину процеса. Могућност коришћења оба адсорбента, NC-PEG и NC-PEG/FO, током више циклуса адсорпције/десорпције представља позитиван индикатор за разматрање њихове примене.

(Примљено 29. маја, ревидирано 14. јуна, прихваћено 15. јуна 2016)

REFERENCES

1. L. Järup, *Brit. Med. Bull.* **68** (2003) 167
2. P. B. Tchounwou, C. G. Yedjou, A. K. Patlolla, D. J. Sutton, *EXS* **101** (2012) 133
3. P. Ravenscroft, H. Brammer, K. Richards, *Arsenic Sollution: A Global Synthesis*, John Wiley & Sons, London United Kingdom, 2009
4. S. Hokkanen, E. Repo, M. Sillanpää, *Chem. Eng. J.* **223** (2013) 40
5. D. Lakherwal, *Adsorption of Heavy Metals: A Review*, *IJERD* **4** (2014) 41
6. O. Kononova, N. Karplyakova, E. Duba, *J. Serb. Chem. Soc.* **80** (2015) 1149
7. S. Lazarević, I. Janković-Častvan, B. Jokić, Đ. Janaćković, R. Petrović, *J. Serb. Chem. Soc*. **81** (2016) 197
8. A. Buekens, N. N. Zyaykina, *Pollution Control Technologies: Adsorbents and adsorption processes for pollution control*, Vol. 2. Eollss Publishers Co. Ltd., Oxford, UK, 2009
9. W. M. Hosny, A. K. A. Hadi, H. El-Saied, A. H. Basta, *Polym. Int.* **37** (1995) 93
10. R. Saliba, H. Gauthier, R. Gauthier, M. Petit-Ramel, *J. Appl. Polym. Sci.* **75** (2000) 1624
11. X. Yu, S. Tong, M. Ge, L. Wu, J. Zuo, C. Cao, W. Song, *J. Environ. Sci.* **25** (2013) 933
12. G. Siqueira, J. Bras, A. Dufresne, *Polymers* **2** (2010) 728
13. E. C. da Silva Filho, J. C.P. de Melo, M. G. da Fonseca, C. Airoldi, *J. Colloid Interface Sci.* **340** (2009) 8
14. J. Zhang, T. J. Elder, Y. Pu, A. J. Ragauskas, *Carbohyd. Polym.* **69** (2007) 607
15. W. Shen, S. Chen, S. Shi, X. Li, Xi. Zhang, W. Hu, H. Wang, *Carbohyd. Polym.* **75** (2009) 110
16. X. Zhao, G. Zhang, Q. Jia, C. Zhao, W. Zhou, W. Li, *Chem. Eng. J.* **171** (2011) 152
17. P. Lu, Y-L. Hsieh, *Carbohyd. Polym.* **82** (2010) 329
18. N. Đorđević, A. D. Marinković, J. B. Nikolić, S. Ž. Drmanić, M. Rančić, D. V. Brković, P. S. Uskoković, *J. Serb. Chem. Soc.* **81** (2016) 589
19. U. Schwertmann, *ron Oxides in the Laboratory, Preparation and Characterization*, 2nd ed., Wiley-VCH Verlag GmbH, Weinheim, Germany. 2000
20. M. Iqbal, N. Iqbal, I.A. Bhatti, N. Ahmad, M. Zahid, *Ecol. Eng.* **88** (2016) 265
21. A. Witek-Krowiak, K. Chojnacka, D. Podstawczyk, A. Dawiec, K. Pokomeda, *Bioresour. Technol.* **160** (2014) 150
22. S. A. Jafari, S. Cheraghi, M. Mirbakhsh, R. Mirza, A. Maryamabadi, *CLEAN – Soil Air Water* **43** (2015) 118
23. S.A. Jafari, S. Cheraghi, M. Mirbakhsh, R. Mirza, A. Maryamabadi, *CLEAN –Soil, Air, Water*, **43** (2014) 118
24. G. D. Vuković, A. D. Marinković, S. D. Škapin, M. T. Ristić, R. Aleksić, A. Perić-Grujić, P. S. Uskoković, *Chem. Eng. J.* **173** (2011) 855
25. J. S. Markovski, D. D. Marković, V. R. Dokić, M. Mitrić, M. D. Ristić, A. E. Onjia, A. D. Marinković, *Chem. Eng. J.* **237** (2014) 430
26. K. Taleb, J. Markovski, M. Milosavljević, M. Marinović-Cincović, J. Rusmirović, M. Ristić, A. Marinković, *Chem. Eng. J.* **279** (2015) 66
27. Z. Veličković, G. Vuković, A. Marinković, M.-S. Moldovan, A. Perić-Grujić, P. Uskoković, M. Ristić, *Chem. Eng. J.* **181** (2012) 174
28. G. D. Vuković, A. D. Marinković, M. Čolić, M. Đ. Ristić, R. Aleksić, A. A. Perić-Grujić, P. S. Uskoković, *Chem. Eng. J.* **157** (2010) 238
29. M. A. Karimi, M. Kafi, *Arab. J. Chem.* **8** (2015) 812
30. P. Lakshmipathiraj, B. R. V. Narasimhan, S. Prabhakar, G. Bhaskar Raju, *J. Hazard. Mater., B* **136** (2006) 281
31. S. Glasston, K. J. Laidler, H. Eyring, *The Theory of Rate Processes*, McGraw-Hill, New York, USA, 1941.